

**UNIFIED INTERPOLATION MODELS
FOR
3-D OBJECT GENERATION**

by

**Uday G. Gujar
Virendra C. Bhavsar
Liya Wu**

TR92-066 May 1992

Faculty of Computer Science
University of New Brunswick
P.O. Box 4400
Fredericton, N.B. E3B 5A3

Phone: (506) 453-4566
Fax: (506) 453-3566

E-mail: uday@unb.ca
bhavsar@unb.ca

Abstract

In our earlier work the concept of interpolation has been generalized and a unifying model for generating 3-D objects from two given contours has been presented. The formalization of the unified interpolation model is given in this paper. Both the linear and non-linear unifying models are discussed. The effects of the various elements of the interpolating matrices on the generated object are illustrated. Several theorems about the properties of the generated objects are derived. These models provide versatile techniques for generating a multitude of 3-D objects from given contours.

Keywords: 3-D objects, linear interpolation, non-linear interpolation, parametric modelling, computer aided design.

1. INTRODUCTION

Three dimensional objects are generated using many methods such as rotational and/or translational sweep [1-4], constructive solid geometry [5,6], construction from orthographic views [7,8] and use of blending functions [4,9].

In our earlier work [10] we have generalized the concept of interpolation and used it to generate 3-D objects from two given contours. Various factors that affect the shape of the generated object have been identified and discussed. A unified model for generating 3-D objects from two given contours has been proposed. Two interpolating matrices have been employed for this purpose. The effects of the diagonal elements of these matrices on the generated object have been studied and reported in [10] where the discussion assumes that all the off-diagonal elements are equal to zero.

In this paper we formalize the unified interpolation model and discuss the linear and non-linear cases. All the elements in the interpolating matrices of this model may be non-zero. We illustrate the effects of the various non-zero off-diagonal elements as well as the zero diagonal elements on the generated objects by several examples. Many theorems about the properties of the generated object using this model are presented and proved.

2. UNIFIED INTERPOLATION MODEL

The interpolation between two quantities u and w is given by

$$v = \alpha \cdot u + (1-\alpha) \cdot w \quad \dots (1)$$

for $0 \leq \alpha \leq 1$; we refer to this as the *standard interpolation*. Lofted surfaces [9,11] and Coons surfaces [12] use this standard interpolation.

A set of interpolated quantities, denoted by V , can be obtained by assigning different values to α . It is possible to make α a linear or non-linear function of some parameter, say s . Then

$$v(s) = \alpha(s) \cdot u + \{1 - \alpha(s)\} \cdot w \quad \dots (2)$$

The boundary conditions $v(0)$ and $v(1)$ are linear combinations of u and w for linear as well as non-linear $\alpha(s)$. Depending upon the function $\alpha(s)$, the given quantities u and w may or may not be present in the interpolated set, V , of quantities. Thus the interpolation discussed above gives rise to interpolation, partial interpolation, extrapolation or a combination. We refer to this as the *generalized interpolation* [10].

The concept of interpolation can be applied to generate 3-D objects. We start with two given contours, C_1 and C_2 , each represented by a set of M points. These points are selected using any of the techniques such as equiangular, equidistant, random, multiple occurrences etc. given in [10]. Consider two corresponding points p_m^1 and p_m^2 on C_1 and C_2 respectively. Each p_m^k , for $k=1, 2$, is represented in cartesian co-ordinates as

$$p_m^k = [x_m^k \quad y_m^k \quad z_m^k]^T \quad \dots (3)$$

where $[A]^T$ denotes the transpose of matrix A . When all of the co-ordinates are functions of some parameter t_k , Eq. (3) becomes

$$p_m^k(t_k) = [x_m^k(t_k) \quad y_m^k(t_k) \quad z_m^k(t_k)]^T \quad \dots (4)$$

These points are used to generate N points using interpolation. This process is repeated for all the M corresponding points, i.e., for $m=1, 2, \dots, M$, on the two given contours.

The X, Y, Z coordinates of a 3-D object generated from the interpolated contours can be represented by

$$X=a_1^1x^1+a_1^2x^2, \quad Y=a_2^1y^1+a_2^2y^2, \quad Z=a_3^1z^1+a_3^2z^2 \quad \dots (5)$$

where, a_i^k , for $k=1, 2$ and $i=1, 2, 3$, are interpolating functions and $p^k=[x^k \ y^k \ z^k]$ for $k=1, 2$, represent all the points on the given contours. Eq. (5) can be compactly represented, in matrix form, as

$$P = A^1 \cdot p^1 + A^2 \cdot p^2 \quad \dots (6)$$

where, $P=[X \ Y \ Z]^T$ and A^k , for $k=1, 2$, are 3×3 matrices with off-diagonal elements equal to zero. The interpolated object is defined by N contours generated from Eq. (6); these generated contours are represented as P^n for $n=1, 2, \dots, N$. Further, P_m^n represents the m^{th} point on the n^{th} generated contour, while P_m represents the set of m^{th} points on all generated contours. The curve joining all these P_m points is referred to as L_m curve. The set of L_m curves is denoted as L set. The elements of A^k in this equation are the interpolating functions which may be linear or non-linear functions of some parameter(s) resulting in linear or non-linear interpolation respectively.

One can clearly observe that a_1^k scale the x coordinates of the given contours to give the X coordinates of the generated object; there is no contribution from the y or z coordinates of the given contours towards the X coordinates of the object. Similar observations can be made about the Y and Z coordinates. We refer to the 3-D object generation process based on Eq. (6) as the *generalized interpolation model*. This model has been extensively studied and reported in our earlier work [10].

In general, we can introduce non-zero elements in the off-diagonal positions of the A^k matrices in Eq. (6). This model is then defined as the *unified interpolation model*.

One can further modify Eq. (6), following the treatment analogous to 3-D homogenous transformations, to obtain the generalized formulation for the interpolated object as

$$\mathcal{P} = \mathcal{A}^1 \cdot p^1 + \mathcal{A}^2 \cdot p^2 \quad \dots (7)$$

where, $\mathcal{P}=[X \ Y \ Z \ H]^T$, $p^k=[x^k \ y^k \ z^k \ 1]^T$ for $k=1, 2$ and \mathcal{A}^k are 4×4 matrices. We refer to the object generation model based on Eq. (7) as the *homogeneous unified interpolation model*.

The interpolating matrices \mathcal{A}^k transform the given contours which in turn determine the shape of the 3-D object. The standard transformation matrices used in computer graphics [4, p. 213] affect the entire 3-D object by carrying out scaling, rotation, shear, translation and perspective projection of the object. The elements of the interpolating matrices have similar effects as those for the elements of the standard transformation matrix with one major difference that the former ones modify the components (i.e. generated contours and the L curves) used to synthesize the object while the latter ones affect the entire object itself.

This paper is devoted to the study of the unified interpolation models. When all the elements of A^k are linear functions of some parameter, s , we get *linear unified interpolation model* whereas when at least one of the elements of A^k is a nonlinear function of s we obtain *non-linear unified interpolation model*.

3. LINEAR UNIFIED INTERPOLATION MODEL

Consider Eq. (6) with elements of A^k , for $k=1, 2$, as linear functions of s , i.e.,

$$a_{ij}^k(s) = e_{ij}^k s + q_{ij}^k \quad \dots (8)$$

where, e_{ij}^k and q_{ij}^k are constants. Combining Eqs. (6) and (8) we get the equation of the object as

$$P = (E^1 \cdot s + Q^1) \cdot p^1(t_1) + (E^2 \cdot s + Q^2) \cdot p^2(t_2) \quad \dots (9)$$

If we vary the parameter s between 0 and 1, Eq. (9) gives two end contours, P^I and P^N , of the object. At $s=0$, the generated contour P^I is given by

$$P^I = Q^1 \cdot p^1(t_1) + Q^2 \cdot p^2(t_2) \quad \dots (10)$$

while at $s=1$, the generated contour P^N is

$$P^N = (E^1 + Q^1) \cdot p^1(t_1) + (E^2 + Q^2) \cdot p^2(t_2) \quad \dots (11)$$

An intermediate contour, P^n , then can be written as

$$P^n = P^N \cdot s + (1-s) \cdot P^I \quad \dots (12)$$

Thus Eqs. (12) and (9) represent the standard interpolation between contours P^I and P^N . The interpolating functions for the individual X , Y and Z coordinates may be different, as such the contours P^I and P^N may not, in general, have any similarity with the given contours C_1 and C_2 . Eqs. (9) and (12) represent the generalized linear interpolation between the given contours C_1 and C_2 ; the generated end contours P^I and P^N form the caps of the generated object.

3.1 Properties

The process of object generation involves selecting two corresponding points p_m^1 and p_m^2 from the given two contours C_1 and C_2 , generating interpolated points using Eq. (9) and connecting the corresponding points on the generated contours by straight lines (assuming linear inter-contour connectivity, see [10]). The curve joining the points $p_m^1, p_m^2, \dots, p_m^N$ is denoted by L_m . The set of all L_m , for $m=1, 2, \dots, M$, is denoted by L .

Theorem 1. When the interpolating functions a_{ij}^1 and a_{ij}^2 , for $i=1, 2, 3$ and $j=1, 2, 3$, are linear functions of some parameter s , all the curves in the set L are straight lines.

Proof. From Eq. (9) we can write the equation of the X coordinates of the points $p_m^1, p_m^2, \dots, p_m^N$ on L_m as

$$\begin{aligned} X &= \left\{ \sum_{k=1}^2 e_{11}^k x^k(t_k) + \sum_{k=1}^2 e_{12}^k y^k(t_k) + \sum_{k=1}^2 e_{13}^k z^k(t_k) \right\} s + \left\{ \sum_{k=1}^2 q_{11}^k x^k(t_k) + \sum_{k=1}^2 q_{12}^k y^k(t_k) + \sum_{k=1}^2 q_{13}^k z^k(t_k) \right\} \\ &= \alpha_1 s + \beta_1 \end{aligned} \quad \dots (13)$$

Similarly, Y and Z coordinates of L_m can be shown to be

$$Y = \alpha_2 s + \beta_2 \quad \dots (14)$$

$$Z = \alpha_3 s + \beta_3. \quad \dots (15)$$

For given contours C_1 and C_2 , α_i and β_i , for $i=1, 2, 3$ become constants for specified values of t_1 and t_2 . Consequently, the curve L_m is a straight line. Thus follows the theorem.

Corollary 1. The principal orthographic projections of L_m are straight lines with the slopes α_2/α_1 , α_3/α_2 and α_1/α_3 in the xy , yz and zx planes respectively.

Proof. The proof follows directly from Theorem 1.

Theorem 2. When the interpolating functions a_{ij}^1 and a_{ij}^2 , for $i=1, 2, 3$ and $j=1, 2, 3$ are linear functions of some parameter s , the distance D_m^n between P_m^n and P_m^{n+1} is proportional to the increment in parameter s .

Proof. D_m^n can be written as

$$D_m^n = \{ (X_m^{n+1} - X_m^n)^2 + (Y_m^{n+1} - Y_m^n)^2 + (Z_m^{n+1} - Z_m^n)^2 \}^{1/2} \quad \dots (16)$$

$$= (s_{n+1} - s_n) \{ (\alpha_1)^2 + (\alpha_2)^2 + (\alpha_3)^2 \}^{1/2}. \quad \dots (17)$$

Since α_1 , α_2 and α_3 are constants, D_m^n is directly proportional to the increment in parameter s , proving the theorem.

Remark. If the increments to s are equal then the distances between all pairs of consecutive generated points on L_m are equal. Consequently, the distance between any two consecutive points on any of the principal orthographic projections of L_m is also equal to a constant.

3.2 Examples

We illustrate the use of linear unified interpolation model by several examples. In all these examples we generate various 3-D objects using the same two given contours, namely a circle and a square. The objective is to illustrate the effects of the various elements of the interpolating matrices on the shape of the generated objects as well as the theorems. These examples demonstrate a rich class of objects that can be generated from the same two given contours. One can use many other types of given contours such as a

star, Lissajous figure, ellipse, n -sided polygon. Such contours have been used for generating 3-D objects using generalized interpolation model in [10]. In all the examples given in this paper we show four views; the left-top is the top view (xy plane), the left-bottom is a front view (xz plane), the right-bottom is a side view (yz plane) and the right-top is an isometric view [2,3].

Consider the circle and the square as the given two contours, defined by the following parametric equations:

C_1 : Circle

$$x=\cos(t_1), \quad y=\sin(t_1), \quad z=10, \quad 0 \leq t_1 \leq 2\pi \quad \dots (18)$$

C_2 : Square

$$x=5 \cos(t_2) \cdot |\cos(t_2)|, \quad y=5 \sin(t_2) \cdot |\sin(t_2)|, \quad z=0, \quad 0 \leq t_2 \leq 2\pi \quad \dots (19)$$

We generate the objects by setting $t_1 = t_2 = t$. The increment for t is chosen to be $\pi/10$ so that every contour, given as well as generated, is represented by 21 points (i.e. $M=21$). Note that the first and the last points are the same. Each object is constructed by generating 9 contours (i.e. $N=9$).

Figure 1 shows the object generated using Eq. (9) with the following values of interpolating matrices:

$$E^1=I, \quad Q^1=0, \quad E^2=-I, \quad Q^2=I \quad \dots (20)$$

where I is the identity matrix. This represents a case where diagonal elements of A^1 are s and those of A^2 are $(1-s)$, i.e., the use of the generalized interpolation model. Therefore caps of the generated object are the given contours as can be clearly seen. All the curves in the set L are straight lines as given by Theorem 1. Further the distance between any

two consecutive generated contours is constant due to constant increment in parameter s , illustrating Theorem 2.

The effect of the introduction of a non-zero off-diagonal element, s , in the interpolating matrices, given by Eq. (20), is illustrated in Fig. 2. The objects in Figs. 2(a) - (d) are generated by setting one of the off-diagonal elements of A^l to s , i.e., the shearing effect is due to the circle. For Fig. 2(a), $a_{12}^l = s$, i.e., the x -coordinates are modified with the value of s multiplied by the corresponding y -coordinates. Thus the xy and xz views are changed and the yz view remains the same. Modification of the given circle into an ellipse can be clearly observed. In Fig 2(b), $a_{13}^l = s$, hence the xy and xz views are altered. Here the x -coordinates are modified with s ; since z is a constant ($=10$) for C_1 , top cap remains the circle except it is translated in the x -direction. The yz view remains the same as in Fig. 1. Note that the object in this figure is scaled smaller in size compared to that in Fig. 1 to accommodate all the views in the same size viewport. Effect of setting $a_{21}^l = s$ is illustrated in Fig. 2(c). For Fig. 2(d), $a_{31}^l = s$ i.e. z -coordinates are affected by the factor sx . Consequently as value of s increases from 0 to 1 the tilt in the generated contours is apparent; the xy view is unaffected.

For the object represented in Fig. 3, we have introduced non-zero elements equal to 0.1 in all the off-diagonal elements in E^l (keeping the diagonal elements unity) in Eq. (20). All the views of the object are affected by the shear introduced for all the x - y - z coordinates. In addition, since the shear is applied to the z -coordinates, the generated contours are no longer parallel to the x - y plane. The bottom cap is the same as the given square.

The objects given in Fig. 4 are generated by introducing a constant term in one of the off-diagonal elements in A^1 . In Fig.4(a), $a_{12}^1=2$, i.e., the x -coordinates are modified by a constant multiplied by the corresponding y -coordinates. For Fig.4(b), $a_{13}^1=2$ i.e. the x -coordinates are modified by two times the z -coordinates, which are equal to a constant 10 in our case, of the points on the first contour. Thus the x -coordinates are translated by 20. Since the graphics package [2,3] centers the object in the viewport, the translation effect is eliminated and the object appears to be the same as shown in Fig. 1. The value of the element a_{21}^1 is set to 2 for Fig. 4(c) while $a_{31}^1=2$ for Fig. 4(d).

The z -coordinates are changed with two times the x -coordinates of the points on the given circle in Fig. 4(d). Thus, none of the generated contours for the objects in Figs. 4(a), (c), and (d) resemble the given contours.

Effects of multiple constant shear (i.e., off-diagonal) elements are shown in Figs. 5(a) and (b). For Fig. 5 (a), we use $a_{31}^1=a_{32}^1=2$, whereas all the off-diagonal elements of A^1 are set to 2 for Fig. 5(b).

We show some further effects of the non-zero off-diagonal elements in the interpolating matrices in Fig. 6. We introduce shear effect for both the given contours by setting $a_{31}^1=s$ and $a_{12}^2=(1-s)$ in Fig. 6(a). For Fig. 6(b) one shear element, a_{31}^1 , is s for the first contour while one shear element (a_{12}^2) is a constant (0.5) for the second contour. The effect of a negative constant off-diagonal element, $a_{12}^1=-2$, is illustrated in Fig. 6(c); this object is the same as the one given in Fig. 4(a) except that it is rotated by 90° about the z -axis.

All the objects presented so far are generated with non-zero diagonal elements in A^1 and A^2 . The diagonal elements for both A^1 and A^2 are set to zero while all the off-diagonal elements of A^1 and A^2 are set to s and $(1-s)$ respectively for the object shown in Fig. 7.

For Fig. 8 we use the following interpolating matrices:

$$A^1 = \begin{bmatrix} 0.9 & 0.1 & 0.3 \\ 0.2 & 1 & 0.1 \\ 0.3 & 0.2 & 0.9 \end{bmatrix} s + \begin{bmatrix} 0.1 & 0.2 & 0.1 \\ 0.3 & 0.1 & 0.2 \\ 0.2 & 0.3 & 0.2 \end{bmatrix} \quad \dots (21a)$$

$$A^2 = \begin{bmatrix} 0.8 & 0.1 & 0.2 \\ 0.1 & 0.9 & 0.2 \\ 0.3 & 0.1 & 0.9 \end{bmatrix} (-s) + \begin{bmatrix} 0.9 & 0.2 & 0.1 \\ 0.1 & 0.8 & 0.2 \\ 0.1 & 0.2 & 0.9 \end{bmatrix} \quad \dots (21b)$$

The object is warped in all directions.

In all these figures the curves in the set L are straight lines as given by Theorem 1 and the distance between any two generated consecutive contours along an L_m curve is constant as given by Theorem 2.

4. NON-LINEAR UNIFIED INTERPOLATION MODEL

In the non-linear unified interpolation model at least one element a_{ij}^k of A^k , for $k=1, 2$, in Eq. (6) is a non-linear function of s . In this case the three principal orthographic projections of the curve L_m joining points $p_m^1, p_m^2, \dots, p_m^N$ on the generated contours are straight lines or curves depending upon how many rows of A^k contain non-linear functions. We denote projections of L_m on the $x=0, y=0$ and $z=0$ planes as L_m^x, L_m^y and L_m^z respectively.

4.1 Properties

Consider any two corresponding points p_m^n and p_m^{n+1} on two consecutive generated contours. The X, Y, Z coordinates of p_m^n are

$$X_m^n = \sum_{k=1}^2 a_{11}^k(s_n) \cdot x^k + a_{12}^k(s_n) \cdot y^k + a_{13}^k(s_n) \cdot z^k \quad \dots (22a)$$

$$Y_m^n = \sum_{k=1}^2 a_{21}^k(s_n) \cdot x^k + a_{22}^k(s_n) \cdot y^k + a_{23}^k(s_n) \cdot z^k \quad \dots (22b)$$

$$Z_m^n = \sum_{k=1}^2 a_{31}^k(s_n) \cdot x^k + a_{32}^k(s_n) \cdot y^k + a_{33}^k(s_n) \cdot z^k \quad \dots (22c)$$

The projection L_m^z is a straight line only if the slopes $(Y_m^{n+1} - Y_m^n)/(X_m^{n+1} - X_m^n)$ are the same for $n=1, 2, \dots, N-1$. This is true if the interpolating functions a_{ij}^k , for $\{i=1, 2\}, \{j=1,2,3\}$ and $\{k=1, 2\}$, are linear functions of s ; if any of these interpolating function is non-linear, L_m^z is not a straight line. Similar statements can be made by L_m^x and L_m^y . The curve L_m is a straight line only when all L_m^x, L_m^y and L_m^z are straight lines. Based on this discussion we state the following theorem.

Theorem 3. For non-linear unified interpolation all L_m curves in the set L are, in general, non-linear when at least one of the interpolating functions is non-linear. Further, when two corresponding rows in the interpolating matrices A^1 and A^2 are linear functions of s , although L_m is non-linear, one of its projections, L_m^x, L_m^y or L_m^z is linear.

Theorem 4. If the first two rows of the two interpolating matrices are non-linear functions of s , the shape of the object in the z -direction is proportional to

$$\sum_{k=1}^2 [a_{11}^k(z) x^k + a_{12}^k(z) y^k + a_{13}^k(z) z^k]$$

Proof. In the cylindrical coordinate system (r, θ, z) , when θ is equal to some constant θ_c , the shape of the generated object in the z -direction is given by r as a function of z . In this system

$$\begin{aligned} (r)^2 &= (X)^2 + (Y)^2 \\ &= (X)^2 (1 + \tan^2 \theta_c) \end{aligned} \quad \dots (23)$$

i.e., $r = \lambda X$... (24)

with $\lambda = (1 + \tan^2 \theta_c)^{1/2}$... (25)

Eq. (22a) gives an expression for X as a function s . Since the third rows of A^1 and A^2 are linear functions of s , z is obtained by linear interpolation using Eq. (15). Since α_3 and β_3 in Eq. (15) are constants, s can be expressed as a linear function of z and from Eqs. (22a) and (24) the theorem follows.

Theorem 5. If two rows of A^1 are proportional to a non-linear function $w(s)$, with elements of A^2 proportional to the addition of the corresponding elements of A^1 and some constants, then one of the principal orthographic projections of L_m is a straight line.

Proof. Let

$$a_{ij}^1(s) = \gamma_{ij} \cdot w(s) \quad \dots (26a)$$

$$a_{ij}^2(s) = \delta_{ij} \cdot (a_{ij}^1 + \mu_{ij}) \quad \dots (26b)$$

with $\{i=1, 2\}$, $\{j=1, 2, 3\}$ and γ_{ij} , δ_{ij} , μ_{ij} as constants. Substituting Eq. (26) in Eqs. (22a) and (22b) one can obtain the slope of L_m^z as $(Y_m^{n+1}-Y_m^n)/(X_m^{n+1}-X_m^n)$ for $n=1, 2, \dots, N-1$. In this expression the term $\{w(s_{n+1})-w(s_n)\}$ appears in both the numerator and denominator and gets cancelled, as a result the expression contains only the terms involving γ_{ij} , δ_{ij} and μ_{ij} . Consequently the slope of L_m^z is a constant, i.e. the projection of L_m in the $z=0$ plane is a straight line.

Similar arguments can be made to prove that when $i=1, 3$ in Eq. (26) projection L_m^y is a straight line and when $i=2, 3$, projection L_m^x is a straight line.

Theorem 6. When all the three rows of A^l are proportional to a non-linear function $w(s)$, with the elements of A^2 proportional to the addition of the corresponding elements of A^l and some constants, all the three principal orthographic projections of L_m are straight lines, i.e., L_m is a straight line.

Proof. The proof directly follows as the combination of the three cases discussed in the proof of Theorem 5.

4.2 Examples

In this section we give sample objects generated using the non-linear unified interpolation model. For all these objects the two given contours are the circle and the square defined by Eqs. (18) and (19) respectively. Further we use the following non-linearities in all the examples:

$$w_1(s)=\sin^7 (s\pi/2), \quad w_2(s) = \cos^7 (s\pi/2). \quad \dots (27)$$

It is possible to use many other types of non-linearities, as well as the modifying functions, as discussed and illustrated in our earlier work [10].

We now present the cases where non-linearity is introduced in the diagonal element(s) of A^1 and A^2 . The shear effects by non-zero off-diagonal elements are given followed by illustrations for theorems.

The objects in Fig. 9 are generated using unified non-linear interpolation with non-linearity in the diagonal elements of the interpolative matrices and all the off-diagonal elements equal to zero. For Fig. 9(a) the diagonal elements of A^1 and A^2 are:

$$a_{11}^1 = w_1(s), \quad a_{22}^1 = a_{33}^1 = s, \quad a_{11}^2 = a_{22}^2 = a_{33}^2 = (1-s). \quad \dots (28)$$

Thus only one element is non-linear. The curves in the set L are all non-linear. However, since the second and third rows of A^1 and A^2 are linear functions of s , the projections of the L curves in the side view turn out to be straight lines as given by Theorem 3. The other two projections of the L curves are non-linear. One non-linear element for each contour is introduced for Fig. 9(b) where the a_{ii}^k values are:

$$a_{11}^1 = w_1(s), \quad a_{22}^1 = a_{33}^1 = s, \quad a_{11}^2 = w_1(s), \quad a_{22}^2 = a_{33}^2 = (1-s) \quad \dots (29)$$

Again L^x curves are straight lines in the side view. The object is considerably changed compared to that in Fig. 9(a). Two non-linear elements are introduced for each contour in Figs. 9(c) and (d). The parameters for Fig. 9(c) are

$$a_{11}^1 = a_{22}^1 = w_1(s), \quad a_{33}^1 = s, \quad a_{11}^2 = a_{22}^2 = w_2(s), \quad a_{33}^2 = (1-s) \quad \dots (30)$$

while those for fig. 9(d) are

$$a_{11}^1 = a_{33}^1 = w_1(s), \quad a_{22}^1 = (1-s), \quad a_{11}^2 = a_{33}^2 = w_2(s), \quad a_{22}^2 = (1-s). \quad \dots (31)$$

The L curves are again non-linear. The L^z projections in the top view are linear since the slopes of the components of the L_m^z curve turn out to be constant due to the specific nature

of the interpolating matrices and t_1 being equal to t_2 in Eqs. (18) and (19). Fig. 9(d) is quite different compared to Fig. 9(c). Since the non-linearity is used for the z -coordinates, the spacing between the generated contours in Fig. 9(d) is not constant as is the case for Figs. 9 (a) - (c).

The shear effects of linear as well as non-linear off-diagonal elements are depicted in Fig. 10. For Fig. 10 (a) the diagonal elements are the same as the ones given in Eq. (28) for Fig. 9(a), in addition $a_{12}^1 = w_1(s)$ with all the other off-diagonal elements equal to zero. One can observe the shearing effect in the x -coordinates of the object in Fig. 9(a). The side views in Figs. 9(a) and 10(a) are the same, since y and z coordinates are unaffected. Linear two element shear for the given circle is used for Fig. 10(b). The diagonal elements for Fig. 10(b) are the same as in Eq. (30) used for Fig. 9(c) while the two off-diagonal elements a_{12}^1 and a_{13}^1 are equal to s with all other off-diagonal elements being zero. The shearing effect on the x -coordinates can be clearly seen in the top and front views. The side view remains the same as in Fig. 9(c); the size of this view is smaller due to the scale change by the graphics package (as explained for Fig. 2(b)). The diagonal elements for the object in Figs. 10(c) and (d) are again the same as in Eq. (30) used for Fig. 9(c). Linear one element shear for each contour is used for Fig. 19(c), while constant two element shear for the given circle is used for Fig. 10(d). The non-zero off-diagonal elements are $a_{12}^1 = s$, $a_{12}^2 = (1-s)$ for Fig. 10(c) and $a_{12}^1 = a_{13}^1 = 2$ for Fig. 19(d). The side views in these two figures are the same as that in Fig. 9(c).

We construct the interpolating matrices to satisfy the conditions in Theorem 5 to generate Fig. 11(a). In this case the interpolating matrices are

$$A^1 = \begin{bmatrix} 0.9w_1(s) & 0.1w_1(s) & 0.09w_1(s) \\ 0.1w_1(s) & 0.95w_1(s) & 0.07w_1(s) \\ 1 & s & s \end{bmatrix} \quad \dots (32a)$$

$$A^2 = \begin{bmatrix} 0.9(0.9w_1(s)+0.9) & 0.08(0.1w_1(s)+0.08) & 0.05(0.09w_1(s)+0.07) \\ 0.1w_1(s)+0.01 & 0.95w_1(s)+0.95 & 0.07w_1(s)+0.07 \\ 0 & 0 & 1-s \end{bmatrix} \quad \dots (32b)$$

and therefore L^2 curves in the top view are straight lines.

To generate the object shown in Fig. 11(b) we use the following interpolating matrices:

$$A^1 = \begin{bmatrix} 0.9 & 0.1 & 0.09 \\ 0.1 & 0.95 & 0.07 \\ 0.1 & 0.01 & 0.9 \end{bmatrix} \cdot w_1(s) \quad \dots (33a)$$

$$A^2 = 0.1 \begin{bmatrix} 9.5(0.9w_1(s)+0.9) & 0.8(0.1w_1(s)+0.08) & 0.5(0.09w_1(s)+0.07) \\ 0.5(0.1w_1(s)+0.01) & 9.7(0.95w_1(s)+0.095) & 0.2(0.07w_1(s)+0.09) \\ 0.6(0.1w_1(s)+0.01) & 0.1(0.01w_1(s)+0.05) & 9.5(0.9w_1(s)+0.08) \end{bmatrix} \quad \dots (33b)$$

These matrices are chosen to satisfy the conditions given in Theorem 6, as a result the L curves are straight lines.

5. Conclusion

In this paper we have extended our earlier work on interpolation techniques for 3-D object generation. Several properties of the linear and non-linear cases of the unified interpolation model are derived. The effects of the non-zero off-diagonal elements as well as zero diagonal elements are illustrated. Many of the theorems are exemplified. It is demonstrated that these models provide versatile techniques for generating multitude of 3-D objects from given contours. The elements of the interpolating matrices in these techniques have similar effects as those of the elements of the transformation matrix with

one major difference that the former ones modify the components used to synthesize the object while the latter ones affect the entire object itself.

References

1. A.A.G. Requicha, "Representations for rigid solid: Theory, methods, and systems". ACM Comp. Surveys 12(4), 437-464 (Dec. 1980).
2. U.G. Gujar, "3-D graphics in APL: User perspective". TR84-024, School of Computer Science, University of New Brunswick, Fredericton, N.B., Canada., 32 pages (July 1984).
3. U.G. Gujar "A Three Dimensional Wire Frame Graphics System", Proceedings of APL '87, Dallas, TX, May 10-14, 1987, ACM Press, New York, NY, pp. 1-6 (May 1987).
4. J.D. Foley, A. vanDam, S.K. Feiner and J.F. Hughes, "Computer Graphics: Principles and Practice", Addison-Wesley, Reading, MA (1990).
5. I.C. Braid, "Designing with volumes", Ph.D. Thesis, Computer Lab., University of Cambridge, England (Feb. 1973).
6. M.E. Mortenson, "Geometric Modeling", John Wiley & Sons, New York (1985).
7. I.V. Nagendra and U.G. Gujar, "3-D objects from 2-D orthographic views - A survey", Computer & Graphics, Vol. 12, No. 1, 111-114 (1988).
8. U.G. Gujar and I.V. Nagendra, "Construction of 3D solid objects from orthographic views", Computers and Graphics, Vol. 13, No. 4, pp. 505-521 (1989).
9. R.H. Bartels, J.C. Beatty and B.A. Barsky "An Introduction to Splines for use in Computer Graphics and Geometric Modeling", Morgan Kaufmann, Los Altos, CA (1987).
10. U.G. Gujar, V.C. Bhavsar and N.N. Datar, "Interpolation techniques for 3-D object generation", Computers & Graphics, Vol. 12, Nos. 3/4, pp. 541-555 (1988).
11. D.F. Rogers and J.A. Adams "Mathematical Elements for Computer Graphics", Mc-Graw Hill, New York, NY (1990).
12. S.A. Coons, "Surface patches & B-spline curves", in "Computer Aided Geometric Design" by R.E. Barnhill and R.F. Risenfeld, Eds., Academic Press, New York, NY, pp. 1-16 (1974).

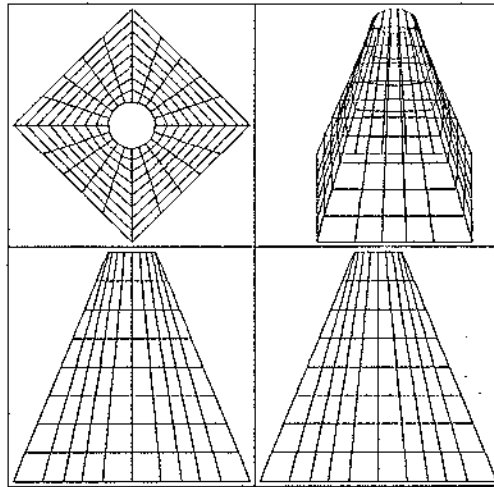
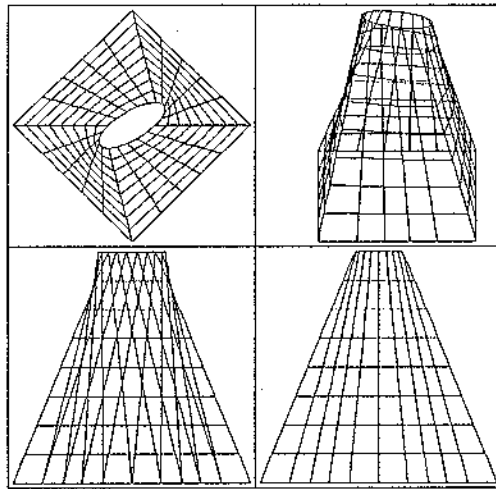
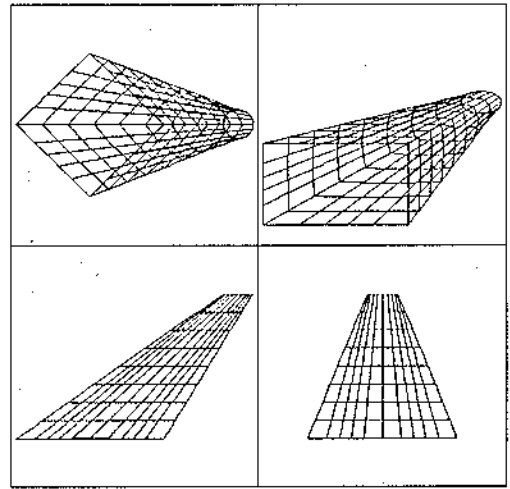


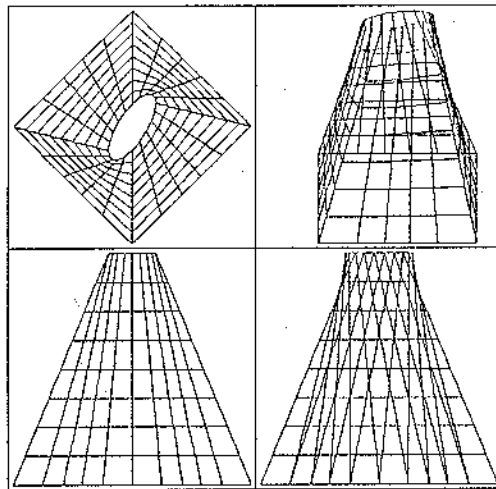
Fig. 1. Unified linear interpolation:
Generalized linear case.



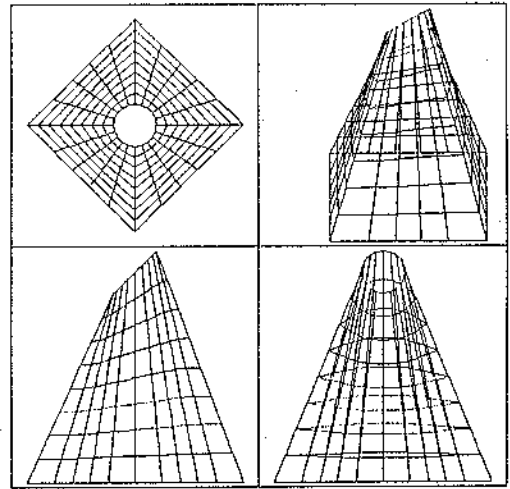
(a) $a_{12}^I = s$.



(b) $a_{13}^I = s$.



(c) $a_{21}^I = s$.



(d) $a_{31}^I = s$.

Fig. 2. Unified linear interpolation:
Single s element shear effect.

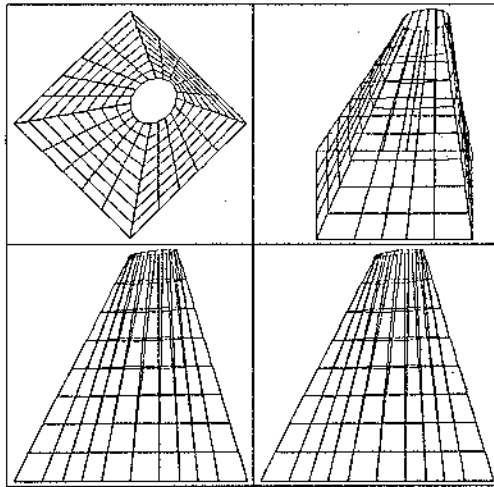
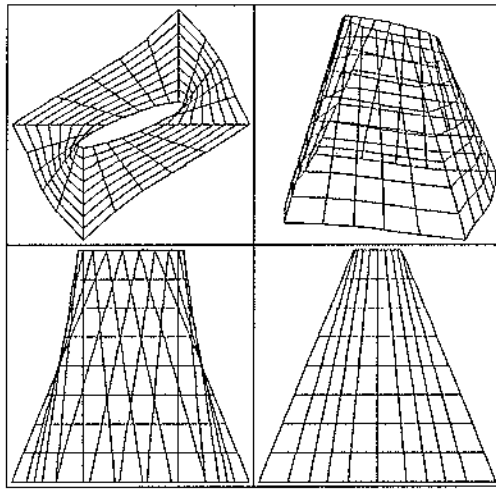
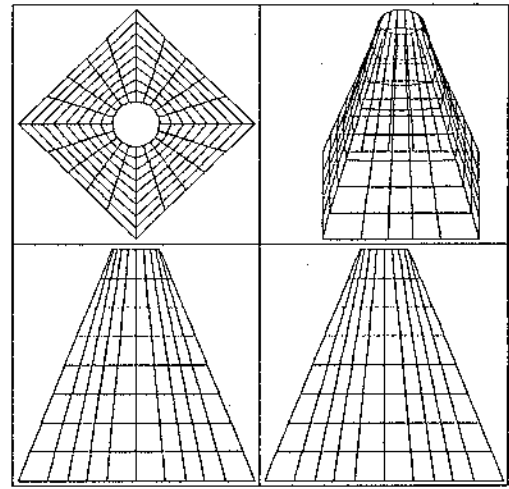


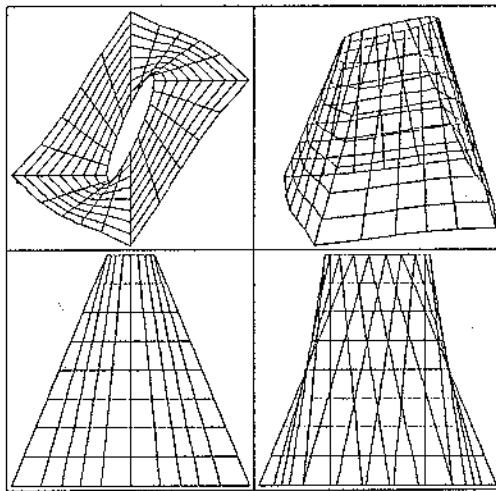
Fig. 3. Unified linear interpolation:
Multiple 0.1s elements shear effect.



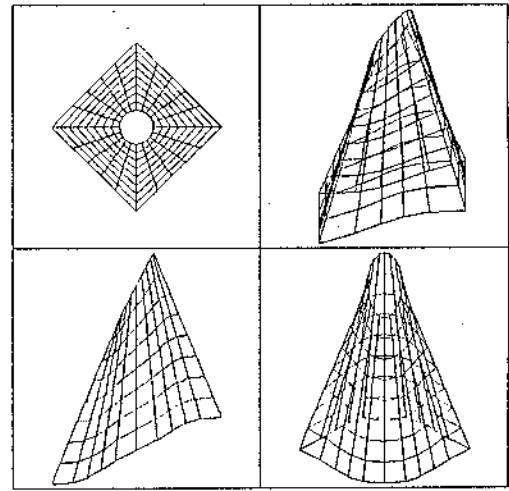
(a) $a_{12}^I = 2$.



(b) $a_{13}^I = 2$.

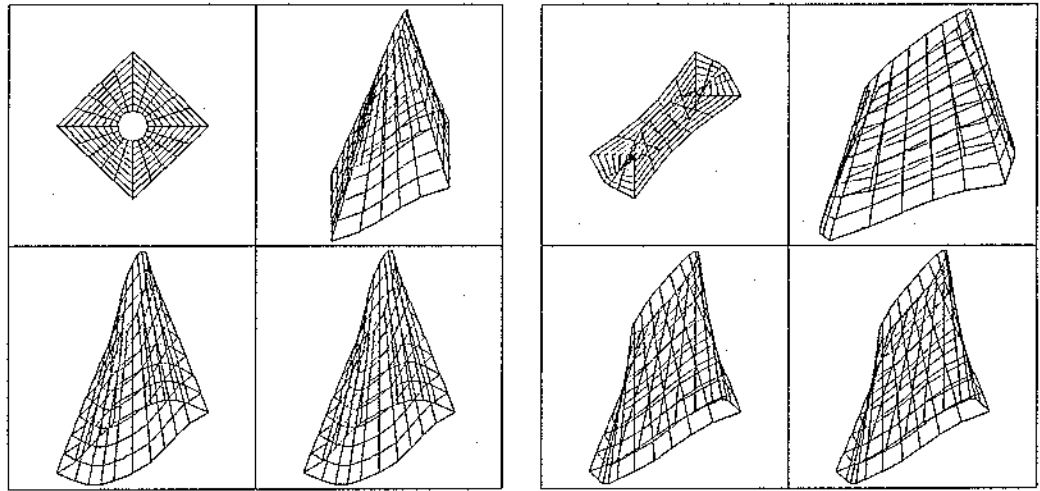


(c) $a_{21}^I = 2$.



(d) $a_{31}^I = 2$.

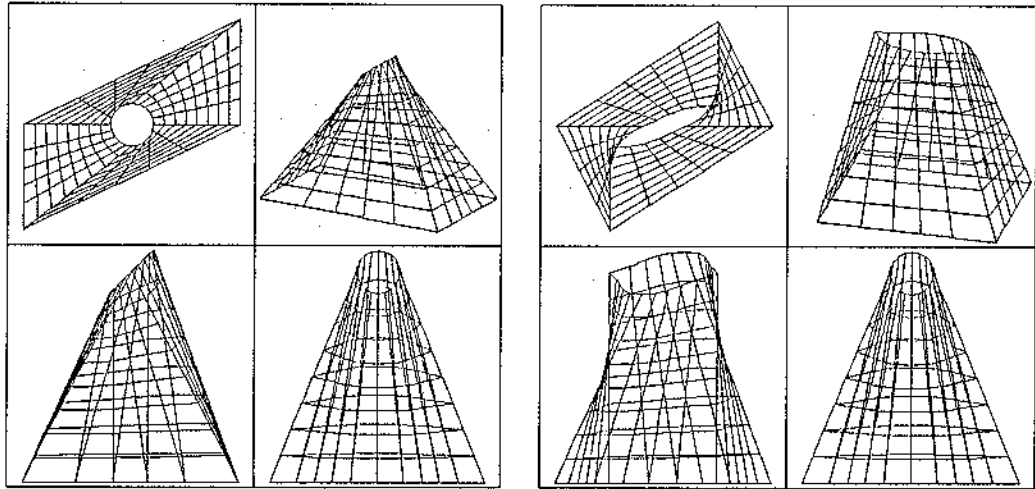
Fig. 4. Unified linear interpolation:
Single constant element shear effect.



(a) $a_{31}^1 = a_{32}^1 = 2$.

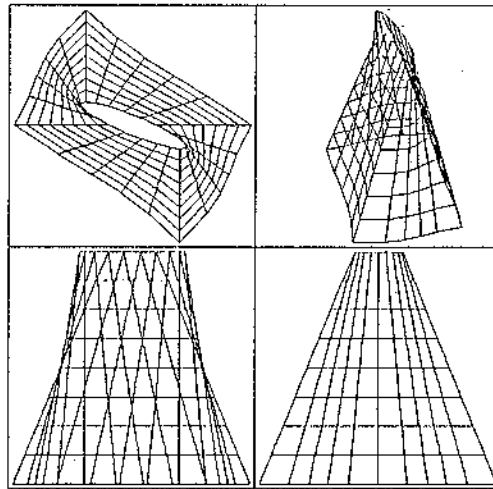
(b) All off-diagonal elements of $A^1 = 2$.

Fig. 5. Unified linear interpolation:
Multiple constant element shear effect.



(a) $a_{31}^1 = s$ and $a_{12}^2 = (1-s)$.

(b) $a_{31}^1 = s$ and $a_{12}^2 = 0.5$.



(c) $a_{12}^1 = -2$.

Fig. 6. Unified linear interpolation:
Miscellaneous effects.

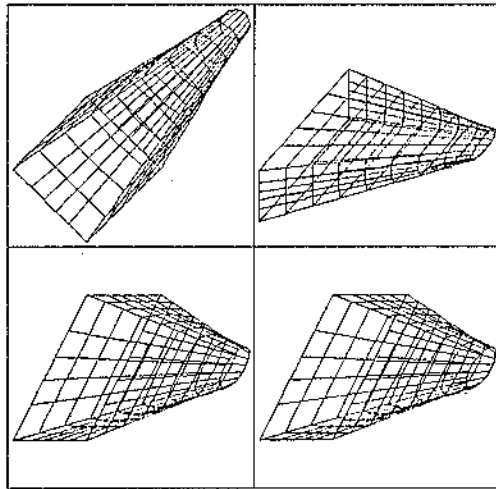


Fig. 7. Unified linear interpolation:
Zero diagonal elements.

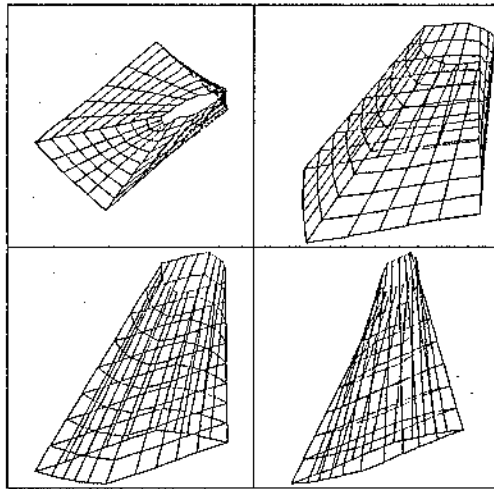
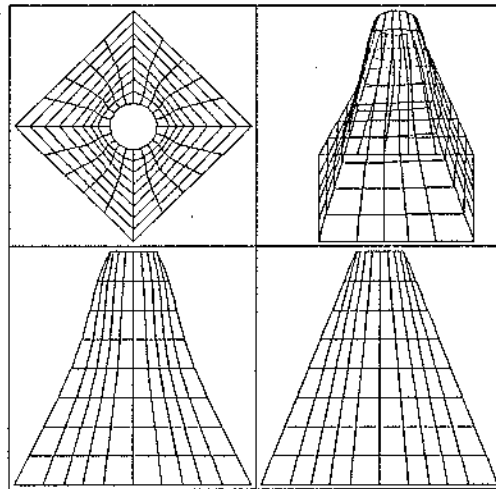
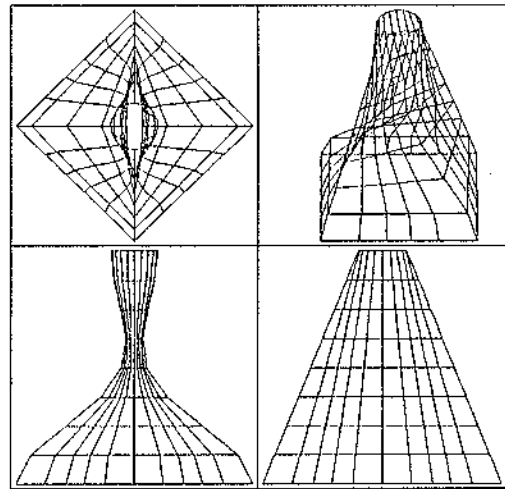


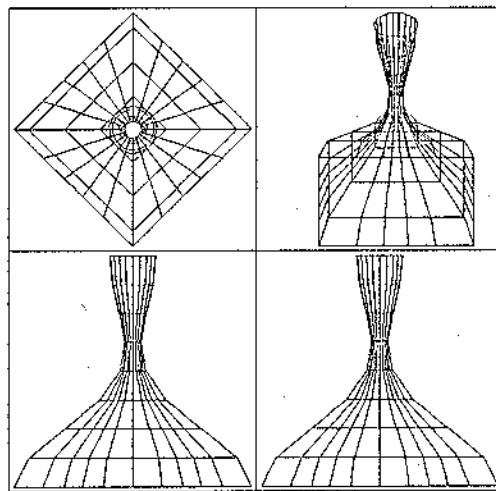
Fig. 8. Unified linear interpolation:
All non-zero elements.



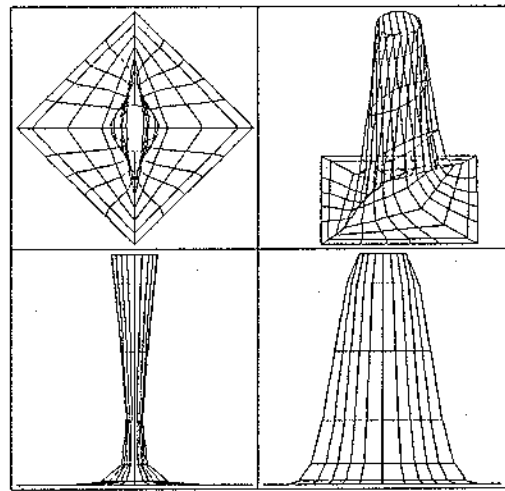
(a) One non-linear element.



(b) One non-linear element for each contour.

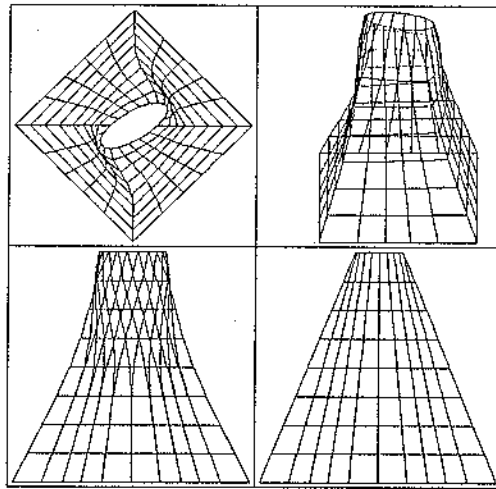


(c) Two non-linear elements for each contour (a_{11}^k and a_{22}^k).

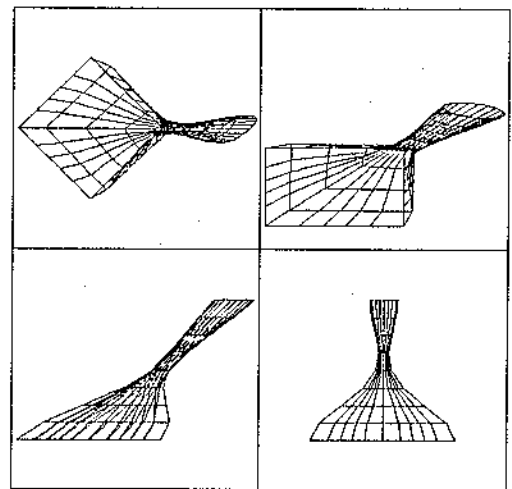


(d) Two non-linear elements for each contour (a_{11}^k and a_{33}^k).

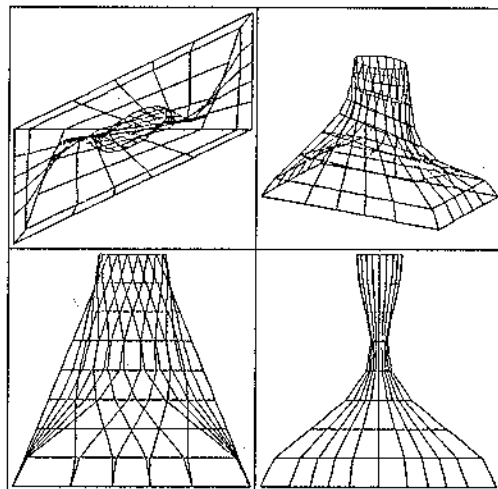
Fig. 9. Unified non-linear interpolation:
Non-linear diagonal element(s).



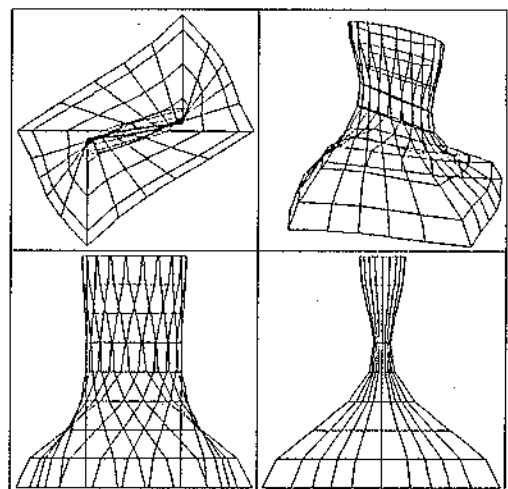
(a) Non-linear single element shear for one contour.



(b) Linear two element shear for one contour.

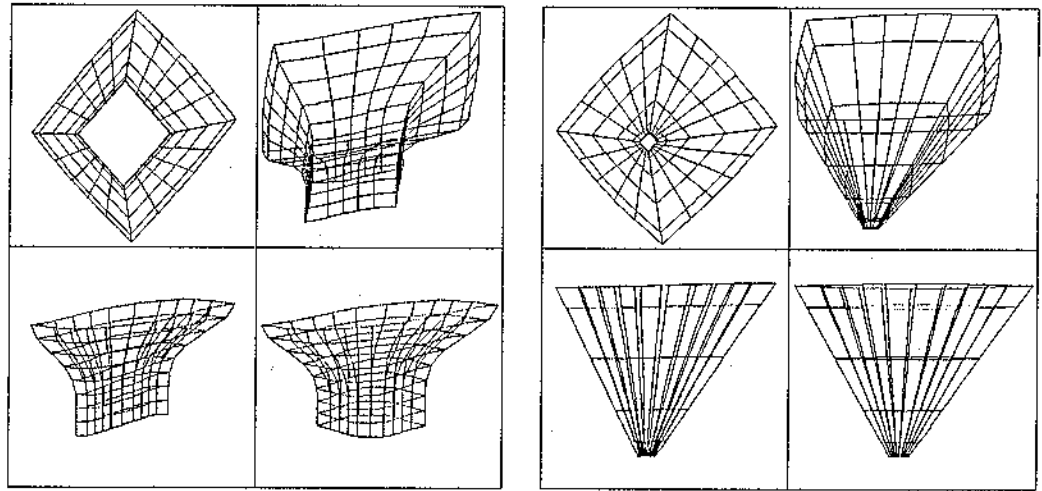


(c) Linear one element shear for each contour.



(d) Constant two element shear for one contour.

Fig. 10. Unified non-linear interpolation:
Shear effects.



(a) Theorem 5.

(b) Theorem 6.

Fig. 11. Unified non-linear interpolation:
Illustrations of theorems.